# A MARKOV MODEL FOR BILLIARDS

E. Shaw[1], H. Sigurgeirsson[2] and A.M. Stuart[3]

*October 2004*

**Abstract**

We describe a simple Markov model for the motion of a tagged particle within a billiard system of $n$ identical spherical particles. The model is based on re-sampling all particle position and velocities from the Maxwell-Boltzmann distribution (except those of the tagged particle itself) after each collision. This enforces Boltzmann's molecular chaos assumption and leads to a discrete time Markov chain for the velocity of the tagged particle after each collision. For large $n$ the collision times are proven to be approximately exponential, conditional on the current tagged particle velocity; making this exponential approximation leads to a continuous time Markov process for the velocity of the tagged particle.

We perform numerical experiments comparing the properties of the Markov model with the corresponding parameters obtained by a hard-sphere simulation. The agreement is remarkably good for low to moderate densities. We prove that the Markov chain is geometrically ergodic. This shows that a tagged particle placed in a billiard system at equilibrium will itself reach equilibrium, and gives information about the rate at which and manner in which this occurs.

[1]Statistics Department, Warwick University, Coventry, CV4 7AL, England. j.e.h.shaw@warwick.ac.uk

[2]SCCM Program, Stanford University, Stanford, CA94305, USA. Supported by the the Department of Energy under the ASCI program. Current address: Kaupthing Bank, 155 Reykjavík, Iceland. hersir@hersir.com

[3]Mathematics Institute, Warwick University, Coventry, CV4 7AL, England. Supported by the Engineering and Physical Sciences Research Council of the UK. stuart@maths.warwick.ac.uk

## 1 Introduction

Consider the billiards problem in a cube of side length $L$ in $d$ dimensions: $n$ identical spheres travel in a vacuum interacting only through elastic collisions, which occur only when two spheres are in contact.[1] In this paper we study the motion of a tagged particle from such a system. This tagged particle will move along a straight line with constant velocity until it hits one of the other particles. Then its velocity will change, and a few moments later it will be travelling along a different straight line with a different constant velocity. Since the collision is elastic, the velocity after the collision is a known function of the velocity of the two particles before the collision.

Given the initial positions and velocities of all the particles in the system, the subsequent motion of the particle is completely deterministic, and can easily be computed.[2] But if we examine its trajectory it will appear random: as if the length of the time intervals between successive collisions, and the velocities of the impacting particles, are drawn at random from some distribution. It therefore seems natural to model this trajectory by a random process. In the case of an infinite system of such particles on a line it has been proven by Spitzer [24] that, under certain conditions on the (random) initial distributions of the particle positions and velocities, the appropriately scaled motion of a single particle is, in distribution, approximately that of Brownian motion. In Holley [13] this result is extended to the situation where the particle of interest is massive compared with all others; its motion is then close in distribution to that of an Ornstein-Uhlenbeck process. In Durr *et al* [8] the work of Holley is extended to two and three dimensions. For the case of hard spheres of equal mass in dimension two or more, there is, to the best of our knowledge, no proven approximation theorem relating the motion of a single tagged particle to that of a stochastic process. However, for systems where the interaction rules amongst particles are stochastic, results in this direction are proved – see [20] and the references therein.

In this paper we propose modelling the velocity of a tagged hard sphere from the billiards problem in 2D by a piecewise constant Markov process $V$. We do this by assuming the Maxwell-Boltzmann distribution for the untagged particles, refreshing this independently whenever the tagged particle undergoes a collision. This particular form of mean-field assumption leads to a Markov process, for the tagged particle velocity, which is amenable to analysis: we prove that it is geometrically ergodic. Furthermore the derivation of the process highlights some shortcomings in previous models for the

[1] We neglect triple collisions.

[2] Computing it *efficiently*, when $n$ is large, is of course not straightforward; see [22], and the references therein, for a discussion concerning efficient algorithms.

motion of a single tagged particle selected from a gas of identical interacting particles; in particular the inter-collision times are often *assumed* to be exponentially distributed (see [19], page 463 and [7]) whilst we *derive* the fact that the inter-collision times are exponential *conditional* on the current tagged particle velocity. Note, however, that this implies that the unconditional distribution is not exponential if the velocity distribution is Gaussian. Since important quantities, such as Lyapunov spectra, are highly sensitive to the precise distribution of collision times, it is important to have a rational derivation of the collision time distribution.

Figure 1 illustrates the form of Markov process we construct. The process $V$ takes the value $V_k$ in the time interval $[\tau_k, \tau_{k+1})$, where $V_k$ is interpreted as the velocity of the particle in the time interval $[\tau_k, \tau_{k+1})$, $\tau_0 = 0$ and $\tau_k, k \geq 1$ is the time of collision number $k$. Then $X_{k+1} = X_k + V_k(\tau_{k+1} - \tau_k)$ is the position of the particle at collision time $\tau_{k+1}$.

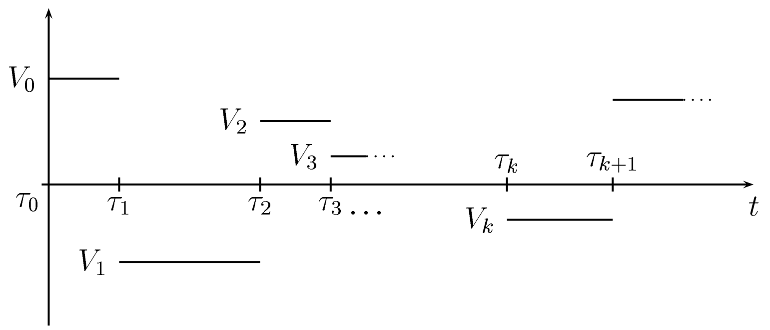


Figure 1: The piecewise constant Markov process. $V$ takes the value $V_k$ in the interval $[\tau_k, \tau_{k+1})$.

In section 2 we describe the model and its derivation. Section 3 contains a proof that the Markov process is geometrically ergodic. In section 4 we sketch how to sample from the distributions required to generate paths of the process. Section 5 contains numerical experiments which compare properties of the Markov model with simulations of the full hard sphere billiards problem. The results show the remarkably good predictive capabilities of the Markov model at low to moderate densities. In section 6 we briefly discuss issues that arise at higher densities. Section 7 contains our conclusions.

Although our derivation of a Markov model utilizes the "molecular chaos" assumption, in the sense that the untagged particles are assumed to be statistically independent of the tagged one, our goals are different from those that led Boltzmann to his celebrated equation. Boltzmann's theory gives the distribution of a large number of identical particles and describes how the whole system approaches the Maxwell-Boltzmann distribution (statistical equilibrium) in time. Our objective is simpler: we wish to describe the statistics of a single particle moving among a large number of particles which are assumed to have *already* reached statistical equilibrium. Thus the untagged particles may be viewed as a heat bath.

A survey of the state of knowledge for the billiards problem in general may be found in [25]; see [23] for recent progress in the study of hyperbolicity for the billiards problem for an arbitrary number of spheres.

There is considerable work concerning the derivation of Markov processes whose law approximates a desired evolution equation. For example, Fournier and Méléard [9, 10] study a piecewise constant stochastic process whose law approximates the solution of Boltzmann's equation, using the ideas of Tanaka [27].

Burshtein, Temkin, Pasterny, and Kivelson have studied Markov chain models for the linear and angular velocity of a single particle in a rarified gas [6, 3, 4, 5, 18, 15, 2]. Most of this work is concerned with developing models valid over a wide range of densities, in particular models valid in situations where the velocity auto-correlation function (VACF) can be negative. This is also the subject of Talbot [26] where, with some probability, collisions are allowed to reverse the sign of some velocity component. Noro, Kivelson, and Tarjus [17] extend Enskog theory to soft potentials, including the effect of environmental crowding due to high density, softness of the potential, and correlations of successive collisions. Our work is primarily concerned with the low density case, where the VACF is positive. However, in contrast to existing works, we do not assume that the collision times are unconditionally exponentially distributed. Rather we derive a distribution for the collision times which is exponential, conditional on the current velocity.

The derivation of stochastic models for components of large complex deterministic systems is a topic of considerable current interest. The work herein provides a concrete and simple example within which such ideas can be tested. We will show that relatively simple, and analytically tractable, stochastic models can be constructed for low density billiards; but we will also show the limitations of our simplistic model at high densities. A survey article describing a variety of situations in which components of large deterministic systems are modelled stochastically is [12].

## 2 The Markov process

Assume that a tagged particle with velocity $V_k$ collides with other particles at random times. Given that a collision has occurred, let $U_{k+1}$ denote the velocity of the impacting particle, and $D_{k+1}$ the unit vector in the direction of contact, see Fig. 2. In an elastic collision, the velocity of the tagged particle after the collision is

$$V_{k+1} = V_k - [(V_k - U_{k+1}) \cdot D_{k+1}]D_{k+1}. \tag{1}$$

If we specify the joint distribution of $U_{k+1}$ and $D_{k+1}$, and pick independently from it for each $k$, then this equation defines a Markov chain $\{V_k\}_{k=1}^{+\infty}$.

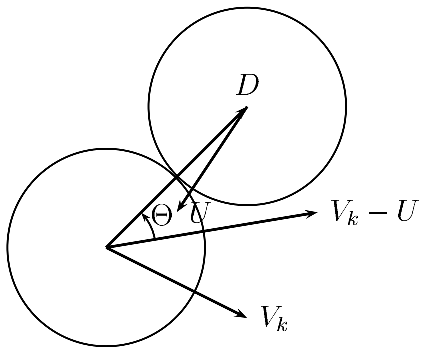


Figure 2: Particle collision. The lower particle is the tagged particle and has velocity $V_k$, and the upper has velocity $U$. $D$ is a unit vector in the direction of contact, and $\Theta$ is the angle it makes with the relative velocity $V_k - U$. For brevity, we omit the subscript $k+1$ here, so $(U, D, \Theta) = (U_{k+1}, D_{k+1}, \Theta_{k+1})$.

It is useful to rewrite Equation (1) in terms of the *angle of impact* $\Theta$, which is the angle between the relative movement of the two particles and the direction of contact, i.e. $\Theta_{k+1}$ is the angle between $V_k - U_{k+1}$ and $D_{k+1}$, see Fig. 2. Equation (1) then becomes

$$V_{k+1} = V_k - \mathcal{A}_{k+1}(V_k - U_{k+1}) = (\mathcal{I} - \mathcal{A}_{k+1})V_k + \mathcal{A}_{k+1}U_{k+1}, \tag{2}$$

where $\mathcal{A}_{k+1} = \mathcal{A}(\Theta_{k+1})$,

$$\mathcal{A}(\Theta) = \cos\Theta\ \mathcal{Q}(\Theta) = \begin{pmatrix} \cos^2\Theta & -\cos\Theta\sin\Theta \\ \cos\Theta\sin\Theta & \cos^2\Theta \end{pmatrix}, \tag{3}$$

and

$$\mathcal{Q}(\Theta) = \begin{pmatrix} \cos\Theta & -\sin\Theta \\ \sin\Theta & \cos\Theta \end{pmatrix}$$

is a rotation by $\Theta$.

To completely specify a Markov chain for the velocities after impact we thus need to specify the joint distribution of $U_{k+1}$ and $\Theta_{k+1}$. To specify the (piecewise constant) stochastic process for velocities as a function of time we need to specify, in addition, the distribution of the inter-collision times $T_{k+1} = \tau_{k+1} - \tau_k$.

This piecewise constant process $V(t)$ may be viewed formally as the solution of the random ODE

$$\frac{dV}{dt} = \sum_{k=1}^{\infty} \delta(t - \tau_k) K_k, \quad V(0) = V_0. \tag{4}$$

Here $\{(T_k, K_k)\}_{k=1}^{\infty}$ is a sequence of random variables with

$$K_k = \mathcal{A}_k[U_k - V(\tau_k^-)].$$

$V(t^-)$ is the left-hand limit of $V(s)$ as $s$ approaches $t$ from below; similarly we will use $V(t^+)$ to denote the right hand limit. The path $V(t)$ is discontinuous only at $t = \tau_k, k \in \mathbb{Z}^+$ and then

$$V(\tau_k^+) - V(\tau_k^-) = K_k,$$

which is equivalent to (2).

In the following three subsections we derive the joint distributions, needed to define (2) and (4), making only two simple statistical assumptions on the distribution of the other particles in the system:

**A1** the particles are uniformly distributed in space, subject to not overlapping;

**A2** their velocities are independent of the positions and are independent and identically distributed amongst different particles, with probability density function $f : \mathbb{R}^d \to \mathbb{R}$.

The two assumptions follow from the work of Boltzmann [1] whose arguments show that, for a system of a large number of hard spheres in statistical equilibrium, the particles are uniformly distributed in space, subject to not overlapping, and their velocities are i.i.d. Gaussian. Sometimes we approximate A1, for small radii, with the simpler assumption of uniformly distributed particles in space.

Having made these assumptions we appeal to statistical mechanics to derive the distributions of $U_{k+1}$, $\Theta_{k+1}$, and $T_{k+1}$, conditional on $V_k$. We then construct a stochastic process by picking a sequence $\{U_k, \Theta_k, T_k\}_{k=1}^{\infty}$ from this joint distribution. Then $V_k$ is given by (2) and $V(t)$ solving (4) is given by

$$V(t) = V_k, \quad t \in [\tau_k, \tau_{k+1}).$$

We will show that, for large $n$, we may take the $T_k$ to be exponential random variables, conditional on $V_k$, and hence that the process $V(t)$ is Markovian. We will also show that, conditional on $V_k$, the random variables $U_{k+1}, \Theta_{k+1}, T_{k+1}$ are independent of one another.

In the next three subsections we drop the subscript $k+1$ on random variables required to specify the Markov chain; we use $\{U, \Theta, T\}$ to denote $\{U_{k+1}, \Theta_{k+1}, T_{k+1}\}$.

## 2.1 Collision times, $T$

In statistical mechanics the distribution of the collision times is often *assumed* to be exponential [19], or it is assumed that the probability of a collision in the next (small) time interval is independent of when the last collision occurred, which in turn gives exponential distribution of the collision times. Our aim, however, is to make no more assumptions than A1 and A2. Hence, in this section, we derive the distribution of the collision times under assumptions A1 and A2. We give a full derivation of the appropriate collision time distribution in one dimension, and then generalize to higher dimension by heuristic arguments.

### One dimension

We first find the next collision time of a stationary particle at the origin in one dimension; see Fig. 3. In the first instance we assume that the particles have no size, i.e. their radius is zero, an assumption that we will relax later. We also assume A1 and A2, namely that the other particles are uniformly distributed on $[-L/2, L/2]$, and their velocities are i.i.d. with pdf $f$.

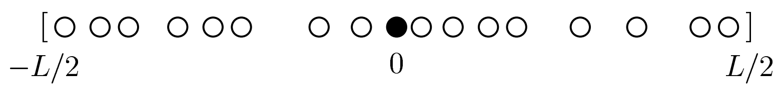


Figure 3: Particles in the interval $[-L/2, L/2]$. The black particle is stationary at the origin.

Let the $n$ other particles have positions and velocities given by the i.i.d. random vectors $\{(P_i, Q_i)\}_{i=1}^n$. The particle at the origin will of course only collide with either of its immediate neighbors, on the left or on the right.

We want to find (i) the time of the next collision, and (ii) the velocity of the impacting particle. To this end note that, in one dimension, when two particles (of zero radius) collide it is as if they pass through each other. Using this interpretation of the dynamics shows that particle $i$ will reach the origin at the time $S_i$ given by

$$S_i = \begin{cases} -P_i/Q_i & \text{if } -P_i/Q_i > 0 \\ \infty & \text{otherwise} \end{cases}$$

and that the first collision therefore occurs at time

$$T = \min\{S_i \mid i = 1, \dots, n\}.$$

Since the untagged particles are assumed to pass through one another, the colliding particle has velocity $Q_j$ where $j$ is the index which minimizes $S_i$ over $i$. We are interested in the distribution of the time $T$ when $n$ is large, for which we use the following lemma whose proof is in the Appendix; see [11] for more results in a similar vein.

**Lemma 2.1 Minimum of positive random variables** *Let* $\{X_i\}_{i=1}^{\infty}$ *be a sequence of positive i.i.d. random variables with distribution function* $F$ *that is differentiable at* 0 *and satisfies* $F'(0) > 0$. *Define* $\{Y_n\}_{n=1}^{\infty}$ *by*

$$Y_n = \min\{nX_i \mid i = 1, \dots, n\}.$$

*Then, as* $n \to \infty$, $Y_n$ *converges weakly to an exponential random variable with parameter* $\lambda = F'(0)$.

Thus the distribution of the minimum of $n$ positive i.i.d. random variables is approximately exponential for large $n$. Using this lemma we get the next theorem, proved in the Appendix. Stated informally the theorem implies that the collision time $T$ is approximately an exponential random variable with parameter $\lambda = n_0\bar{q}$ where $n_0 = n/L$ is the number density of particles. This is what we will use in the following.

**Theorem 2.2** *Let Assumptions A1, A2 hold and assume that the velocities in A2 are* $L^1$ *random variables. For the one-dimensional system described above, let* $Y = nT$ *where* $T$ *is the collision time. Then* $Y$ *converges weakly, as* $n \to \infty$, *to an exponential random variable with parameter* $\bar{q}/L$, *where*

$$\bar{q} := \int |q| f(q)\, dq$$

*is the mean speed of the particles.*

In the above we made two assumptions that amount to the particles having no size: (i) the collision time is the time it takes a particle to reach the origin; (ii) when two particles collide it is as if they pass through each other. To correct for the first assumption it is natural to let the collision time be the time a particle takes to get within distance $\sigma$ of the origin; this turns out to have no effect on the large $n$ asymptotics of the collision time distribution. Modifying the second assumption to incorporate finite radius does have an effect, however. Denote the positive particle diameter by $\sigma$, and let $K_i$ be the number of particles between particle $i$ (with position $P_i$ and velocity $Q_i$) and the origin. If particle $i$ hits the origin, it has gone $K_i\sigma$ length units of the distance in zero time, so the total time it took to reach the origin is

$$S_i = -\frac{P_i - K_i\sigma}{Q_i}.$$

Under assumption A1, that the particles are uniformly distributed excluding overlap, we can derive the distribution of $K_i$, and compute $F_T'(0)$ as before. This gives that the hitting time is approximately exponentially distributed with rate

$$\lambda = \frac{n_0}{1-\sigma n_0}\bar{q}. \tag{5}$$

See [21, Chapter 5] for details. Note that $\sigma n_0 < 1$ unless all particles are in contact with their neighbors.

### Higher dimensions

To generalize this result to higher dimensions we argue heuristically[3] and write (5) as

$$\lambda = g(n_0)\bar{q}. \tag{6}$$

where $g(n_0)$ is some function of the particle density, such that $g(n_0) \approx \sigma_c n_0$ for small $n_0$ where $\sigma_c$ is the collision cross section of two particles. For $d = 1$, 2, or 3 dimensions we have $n_0 = n/L^d$, and

$$\sigma_c = \begin{cases} 1 & \text{in 1D,} \\ 2\sigma & \text{in 2D,} \\ \pi\sigma^2 & \text{in 3D,} \end{cases}.$$

Equation (6) agrees with the collision rate formula (12.2.7) in [19] in the low density limit. Note however that we have *derived* the exponential distribution, whereas the standard calculation in [19] postulates an exponential distribution and then finds its rate.

[3]However, we have verified numerically that our heuristics give a better fit to hard sphere data than do other assumptions of the form (5).

In the following we assume that the distribution of the inter-collision times $\{T_k\}$, conditional on $V_k = v$, is exponential in the limit as $n \to \infty$ with parameter $\lambda$ given by (6) where now

$$\bar{q} = \int f(q)||q - v||dq$$

is the mean relative speed of the tagged particle with velocity $v$ and the particle with which it collides.

## 2.2 Velocity of the impacting particle, $U$

To find the distribution of $U$, the velocity of the impacting particle, we work in a frame of reference where the tagged particle is at rest, so the velocity of the impacting particle is $U - V_k$. From the previous subsection we see that the *collision rate* (the number of collisions per time unit) of the tagged particle with untagged particles at velocity $u$ is $g(n_0)f(u)||u - v||$. Here $f$ is the pdf for the velocities of the particles. The fraction of {collisions with particles with velocity $u$} to {collisions with all other particles} is therefore

$$f_{U|V_k}(u \mid v) = \frac{g(n_0)f(u)||u - v||}{\int g(n_0)f(w)||w - v||dw} = f(u)\frac{||u - v||}{\bar{v}}.$$

## 2.3 Angle of impact, $\Theta$

Consider a flux of particles with velocity $U$ impacting on the tagged particle with velocity $V_k$, as shown in Fig. 4; see Reif [19], pages 467–468. From the Figure it is clear that $\sin\Theta$, given $U$ and $V_k$, should be uniformly distributed in $[-1, 1]$. Since this does not involve the value of $U$, $\Theta$ and $U$ are in fact independent, so $\Theta \sim \arcsin(\mathcal{U}[-1, 1])$ and hence the pdf is

$$f_\Theta(\theta) = \frac{1}{2}\cos\theta.$$

## 2.4 Summary

To summarize, the model is a piecewise constant Markov process taking the value $V_k$ in the interval $[\tau_k, \tau_{k+1})$ with

$$V_k = (\mathcal{I} - \mathcal{A}_k)V_{k-1} + \mathcal{A}_k U_k, \tag{7}$$

$$\mathcal{A}_k = \begin{pmatrix} C_k^2 & -C_k S_k \\ C_k S_k & C_k^2 \end{pmatrix},$$

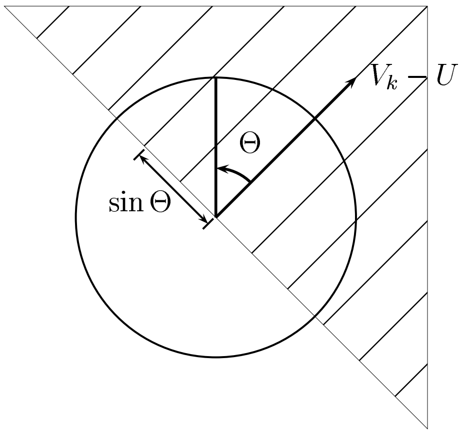


Figure 4: Angle of impact. The incident lines represent a "flux" of particles with velocity $U$ impacting on the tagged particle with velocity $V_k$.

where $\{S_k\}_{k=1}^{+\infty}$ are an i.i.d. sequence uniform in $[-1, 1]$, $C_k = \sqrt{1 - S_k^2}$, and the $\{U_k\}_{k=1}^{+\infty}$ are an i.i.d. sequence independent of the $\{S_k\}$ with conditional pdf

$$f_{U_k|V_{k-1}}(u|v) = \frac{||u - v||}{\bar{v}} f(u).$$

Here $f$ is the equilibrium velocity distribution. The inter-collision times $\{T_k\}_{k=1}^{+\infty}$ are independent exponential variables with parameter

$$\lambda_k = g(n_0)\bar{V}_{k-1}.$$

Recall that we have predicted the analytic form of $g$ at small number density, but that we will fit it to numerical data for higher densities. Here we use bar to denote mean speed, in the equilibrium distribution, relative to the quantity under the bar,

$$\bar{v} = \int f(u)||u - v||du.$$

Then $V$ is a continuous time Markov process because the inter-collision times are conditionally exponential. Note that $T_{k+1}$ and $V_{k+1}$ are independent conditional on $V_k$, because $V_{k+1}$ is determined by $U_{k+1}, \Theta_{k+1}$ which are independent of $T_{k+1}$.

# 3 Ergodicity

A natural question to ask is whether the Markov chain for $\{V_k\}_{k=0}^{+\infty}$ is ergodic. We assume that $f$ is nowhere zero, that it is continuous in $\mathbb{R}^d$ and gives rise to bounded third moments; note that these assumptions hold for the Maxwell-Boltzmann distribution which is the main case of interest. Let $\mathbb{E}$ denote expectation under application of the Markov chain (7). Then Theorem 2.4 in [16] gives geometric ergodicity for the chain in the following sense:

**Theorem 3.1** *The Markov chain $\{V_k\}_{k=0}^{+\infty}$, given by (7), has a unique invariant measure $\pi$. Furthermore, there exist $r < 1$ and $\kappa > 0$ such that*

$$|\mathbb{E}h(V_k) - \pi(h)| \leq \kappa r^k(1 + ||V_0||^2)$$

*for all measurable $h : \mathbb{R}^d \to \mathbb{R}$ with $|h(x)| \leq 1 + ||x||^2$, $x \in \mathbb{R}^d$.*

We let $\mathcal{F}_k$ be the filtration generated by $V_k$ and denote the conditional expectation $\mathbb{E}[X \mid \mathcal{F}_k]$ by $\mathbb{E}_k X$. Let $P_k(x, A)$ denote the $k$-step transition kernel for the Markov chain $\{V_k\}$. To prove Theorem 3.1 it suffices to show that the Markov chain $\{V_k\}_{k=0}^{+\infty}$ has the following three properties [16]:

**Lyapunov function returns to a compact set**

$$\exists R > 0 \text{ and } \lambda \in (0, 1) \text{ such that } \mathbb{E}_k||V_{k+1}||^2 < \lambda||V_k||^2 + R$$

**Uniformly reachable point from within the compact set**

Let

$$C = \left\{ v \in \mathbb{R}^d \;\middle|\; ||v||^2 < \frac{R}{1-\lambda} + \epsilon \right\}.$$

For some $\delta > 0$, $\epsilon > 0$, and $v^* \in C$ there exists $l \in \mathbb{N}$ with the property that

$$P_l\left(v, \mathcal{B}_\delta(v^*)\right) > 0, \quad \forall v \in \bar{C}.$$

**Smoothness of probability densities**

The transition kernel has a density which is jointly continuous. That is,

$$P_k(x, A) = \int_A p_k(x, y) dy$$

and $p_k(x, y)$ is jointly continuous in $x$ and $y$.

In the remainder of this section we show that the Markov chain $\{V_k\}_{k=0}^{+\infty}$ has these three properties, thereby establishing Theorem 3.1.

### 3.1 Return to a compact set

Let $\Theta = \Theta_{k+1}$ and $U = U_{k+1}$. Recall that $\mathcal{A}_{k+1}$ is given by (3) and the angle of impact, $\Theta$, is such that $\sin\Theta$ is uniformly distributed in $[-1, 1]$. We therefore have

$$\mathbb{E}_k[\cos^2\Theta] = 1 - \mathbb{E}_k[\sin^2\Theta] = 1 - \frac{1}{3} = \frac{2}{3}$$

and

$$\mathbb{E}_k[\cos\Theta\sin\Theta] = 0$$

and hence $\mathbb{E}_k\mathcal{A}_{k+1} = \frac{2}{3}\mathcal{I}$, and $\mathbb{E}_k[\mathcal{I} - \mathcal{A}_{k+1}] = \frac{1}{3}\mathcal{I}$.

Now we compute $\mathbb{E}_k||V_{k+1}||^2$. Since $\mathcal{Q}(\Theta)$ is unitary and $\mathcal{A}_{k+1} = \cos\Theta\ \mathcal{Q}(\Theta)$, we have $\mathcal{A}_{k+1}^\top\mathcal{A}_{k+1} = \cos^2\Theta\ \mathcal{I}$, and hence

$$\mathbb{E}_k[\mathcal{A}_{k+1}^\top\mathcal{A}_{k+1}] = \frac{2}{3}\mathcal{I}.$$

It follows that

$$\begin{aligned}\mathbb{E}_k[(\mathcal{I} - \mathcal{A}_{k+1})^\top(\mathcal{I} - \mathcal{A}_{k+1})] &= \frac{1}{3}\mathcal{I},\\ \mathbb{E}_k[(\mathcal{I} - \mathcal{A}_{k+1})^\top\mathcal{A}_{k+1}] &= 0,\end{aligned}$$

so using again that $U$ and $\Theta$ are independent we immediately get

$$\begin{aligned}\mathbb{E}_k||V_{k+1}||^2 &= \mathbb{E}_k||(\mathcal{I} - \mathcal{A}_{k+1})V_k + \mathcal{A}_{k+1}U||^2\\ &= V_k^\top\mathbb{E}_k\left[(\mathcal{I} - \mathcal{A}_{k+1})^\top(\mathcal{I} - \mathcal{A}_{k+1})\right]V_k\\ &\quad + 2V_k^\top E_k\left[(\mathcal{I} - \mathcal{A}_{k+1})^\top\mathcal{A}_{k+1}\right]\mathbb{E}_kU\\ &\quad + \mathbb{E}_k\left[U^\top\mathbb{E}_k\left[\mathcal{A}_{k+1}^\top\mathcal{A}_{k+1}\right]U\right]\\ &= V_k^\top\frac{1}{3}\mathcal{I}V_k + \mathbb{E}_k\left[U^\top\frac{2}{3}\mathcal{I}U\right]\\ &= \frac{1}{3}||V_k||^2 + \frac{2}{3}\mathbb{E}_k||U||^2.\end{aligned}$$

Now we need only to bound $\mathbb{E}_k||U||^2$ independently of $V_k$. Note that

$$\mathbb{E}_k||U||^2 = \frac{1}{\overline{V}_k}\int ||u||^2 f_{U|V_k}(u \mid V_k)\,du = \frac{1}{\overline{V}_k}\int ||u||^2||V_k - u||f(u)du. \quad (8)$$

Using the triangle inequality we get

$$\mathbb{E}_k||U||^2 \leq \frac{1}{\overline{V}_k}\left(||V_k||\int ||u||^2 f(u)du + \int ||u||^3 f(u)du\right)$$

$$= \frac{\|V_k\|}{\overline{V}_k} s^2 + \frac{1}{\overline{V}_k} \kappa^3$$

where $s^2$ and $\kappa^3$ denote the second and third moment of the particle velocity distribution respectively. Using the positivity and continuity of $f$, it is straightforward to show that $\overline{V}_k$ and $\overline{V}_k/\|V_k\|$ are bounded away from zero and hence

$$\mathbb{E}_k \|U\|^2 \leq c_1 s^2 + c_2 \kappa^3,$$

uniformly in $k$.

## 3.2 Uniformly reachable point

We now show that there is a uniformly reachable point within the set $C$. In fact a much stronger statement is true, namely that since $f$ is nowhere zero, any point can be reached from any other point in one step,

$$P\left(v, \mathcal{B}_\delta(v^*)\right) > 0 \quad \text{for all } v, v^* \in \mathbb{R}^d \text{ and } \delta > 0.$$

To see this, note first that

$$\begin{aligned}
\mathbb{P}\left(v, \mathcal{B}_\delta(v^*)\right) &= \mathbb{P}\left\{v - \mathcal{A}(\Theta)(v - U) \in \mathcal{B}_\delta(v^*) \mid V_k = v\right\} \\
&= \mathbb{P}\left\{K_v(U, \Theta) \in \mathcal{B}_\delta(v^*) \mid V_k = v\right\} \\
&= \mathbb{P}\left\{(U, \Theta) \in K_v^{-1}(\mathcal{B}_\delta(v^*)) \mid V_k = v\right\}
\end{aligned}$$

where

$$K_v(u, \theta) = v - \mathcal{A}(\theta)(v - u).$$

$K_v$ is a continuous mapping, so the preimage of $\mathcal{B}_\delta(v^*)$ under $K_v$,

$$K_v^{-1}(\mathcal{B}_\delta(v^*)) = \{(u, \theta) \mid \|v - \mathcal{A}(\theta)(v - u) - v^*\| < \delta\}$$

is an open set. Since $K_v(v^*, 0) = v^*$ this set contains the point $(v^*, 0)$.[4] It is thus a nonempty open set and so has nonzero Lebesgue measure.

The joint distribution of $U$ and $\Theta$ given $V_k = v$ is

$$f_{U,\Theta|V_k}(u, \theta \mid v) = f_{\Theta|V_k}(\theta \mid v) f_{U|V_k}(u|v) = \frac{1}{2} \cos\theta \frac{\|u - v\|}{\bar{v}} f(u).$$

This is continuous in $(u, \theta)$ and is zero only when $u = v$ or when $\theta = \pm\frac{\pi}{2}$, and therefore absolutely continuous with respect to Lebesgue measure on $\mathbb{R}^d \times (-\frac{\pi}{2}, \frac{\pi}{2})$. We conclude that the transition probability from $v$ to $\mathcal{B}_\delta(v^*)$ is non-zero.

[4] $(v^*, 0)$ corresponds to the particle being hit by a particle moving with velocity $v^*$ at an angle such that the two particles exchange velocities in the collision.

### 3.3 Smoothness of probability densities

The transition probabilities can be written

$$P(v,A) = P\{K_v(u,\theta) \in A\} = \iint\limits_{K_v^{-1}(A)} f_{U,\Theta|V_k}(u,\theta|v)\,du\,d\theta = \int\limits_A p(v,w)\,dw$$

where

$$p(v,w) = \sum_{K_v(u,\theta)=w} f_{U,\Theta|V_k}(u,\theta|v) J(u,\theta) \tag{9}$$

and where

$$J(u,\theta) = \begin{vmatrix} \frac{\partial K_{v,1}}{\partial u} & \frac{\partial K_{v,2}}{\partial u} \\ \frac{\partial K_{v,1}}{\partial \theta} & \frac{\partial K_{v,2}}{\partial \theta} \end{vmatrix}$$

is the Jacobian determinant of $K_v$. Now $f_{U,\Theta|V_k}$ is continuous and $K_v$ continuously differentiable so (9) gives that $p$, the density of the transition kernel, is continuous.

# 4 Simulation

There are various quantities that can be used to assess the validity of the proposed Markov model by comparing it to the results of a hard sphere billiards simulation. For this and the next section, we assume that the velocity distribution is given by the Maxwell-Boltzmann distribution $\mathcal{N}(0, s^2 I)$, that is

$$f(v) = \frac{1}{2\pi s^2} \exp\left(-\frac{||v||^2}{2s^2}\right).$$

To simulate the Markov process (7) it suffices to draw repeatedly from the distributions of $U$, $\Theta$, and $T$. The last two are straightforward since $\sin\Theta$ is uniformly distributed and $T$ is exponential with parameter depending only on the current particle velocity.[5] Drawing from $U$ is thus the only non-obvious step.

The procedure by which this is achieved is described in detail in [21]. To summarize, we first get an explicit expression for the pdf of $U$ by finding the joint pdf for the random variables $R = ||U - V||$ and $\Phi = \angle(U - V, V)$, the angle $U - V$ makes with $V$. To sample from this joint distribution we find the marginal distribution of $R$ (with $\Phi$ integrated out) and the conditional distribution of $\Phi$ given $R$; we then first draw from the distribution of $R$, using

[5] In [21] $\bar{V}_k$ is evaluated analytically in the Gaussian case, yielding a closed form expression for this parameter.

the marginal, and then, given the value of $R$, draw from the distribution of $\Phi$, using the conditional. We use the well known rejection method to sample from a distribution with a known pdf.

# 5 Validation

We test the validity of the model in subsection 2.4 by comparing sample path properties calculated from it with the corresponding properties of a single particle imbedded in a full hard sphere interacting billiards calculation. By considering a sequence of experiments at increasing densities we show how the model is good for small densities, and demonstrate how it deteriorates as the density increases.

The Markov model is simulated by the methods described in the previous section. The full hard sphere billiards calculation is performed by the methods overviewed in [22].

## 5.1 Density $\phi = 0.2$

We run a billiards simulation of 504 particles at a density $\phi = 0.2$ for about half a million collisions per particle, for a total of about 125 million collisions. We start with the particles positioned on a regular grid and with initial velocities such that the velocity components are i.i.d. Gaussian with mean 0 and variance 1.

We compare the following statistics:

1. Distribution of $V_k$, the velocity at a collision, Fig. 5.

2. Distribution of $V$, the velocity at fixed increments in time, Fig. 6.

3. Distribution of $T_k$, the inter-collision times, Fig. 7.

4. The velocity autocorrelation function, Fig. 8.

First we test the validity of the Markov chain $\{V_k\}_{k=1}^{+\infty}$ by comparing the distribution of $V_k$ to the velocity at collision from hard sphere billiards simulation. This is shown in Fig. 5, and we see that the two curves are virtually indistinguishable; this distribution is not Gaussian.

The distribution of the particle velocity at fixed increments in time, however, should be Gaussian. We choose a small time interval $\Delta t$, and sample the velocity of a particle every $\Delta t$ time units, and make a histogram of the resulting numbers. In Fig. 6 we compare the distribution obtained from

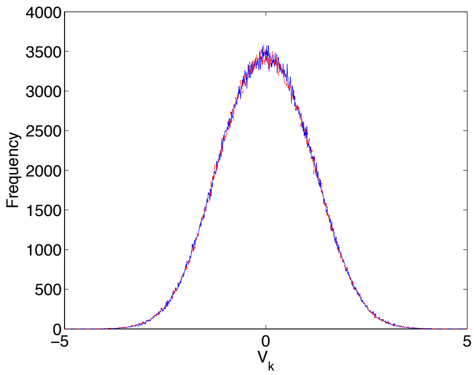


Figure 5: Distribution of $V_k$, particle velocity at collision, obtained from the Markov chain (dashed) and hard sphere billiards simulation (solid) at density $\phi = 0.2$. This distribution is not Gaussian.

simulating the Markov chain with the distribution obtained from the hard sphere billiards simulation and they are indistinguishable.

In Fig. 7, we compare the collision times $T_k$ to the collision time distribution from a hard sphere billiards simulation. The function $g(n_0)$ sets the time-scale of the Markov model; here, and in subsequent experiments at higher density, we estimate its value for $\phi = 0.2$ from the billiards simulation, and set the time unit to one mean collision time. Having made this choice of units, we see that the distribution for the Markov process and the one obtained from hard sphere billiards simulations are almost identical.

The velocity autocorrelation function, VACF, is shown in Fig. 8. As in Fig. 7 the time unit is the mean collision time. Again, the one obtained from the Markov chain is virtually indistinguishable from the true autocorrelation function. This is not be the case at higher densities, though, as it is well known that the true autocorrelation has a negative dip at high densities (see Section 5.3). In contrast, the shape of the autocorrelation function obtained from the Markov chain is independent of the density; the density correction only changes the scale but not the shape. In the Boltzmann theory [1] the VACF decays exponentially in time.

We now return to a more detailed examination of the close agreement seen in Figures 5–7. Each figure can be thought of as showing an expected frequency $E_i$ assuming the Markov model, together with a corresponding observed frequency $O_i$ from the hard sphere billiards simulation, for each 'bin' $i$ used in Figures 5–7. If the observed frequencies $O_i$ were actually drawn independently from the Markov chain model then it is reasonable to

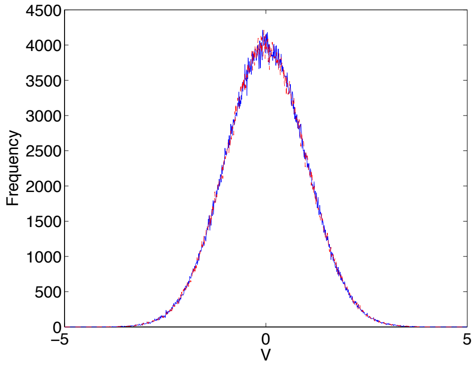


Figure 6: Distribution of $V$, particle velocity, from the Markov chain (dashed) and hard sphere billiard simulation (solid) at density $\phi = 0.2$. This distribution is Gaussian.

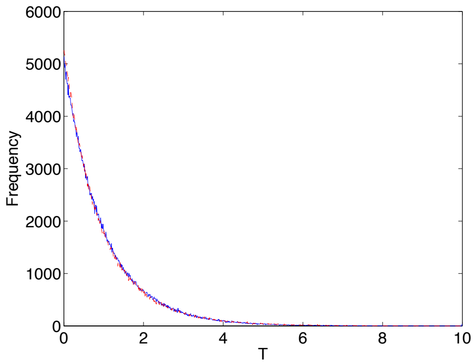


Figure 7: Distribution of $T_k$, inter-collision times, from the Markov chain (dashed) and hard sphere billiards simulation (solid) at density $\phi = 0.2$.

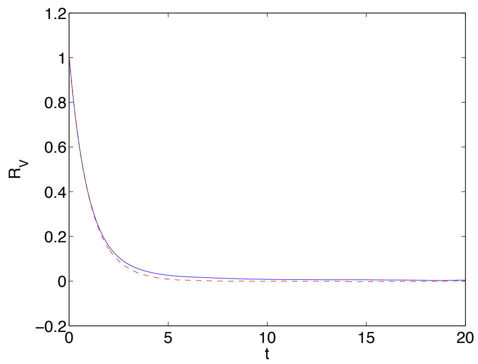


Figure 8: Velocity autocorrelation from the Markov chain (dashed) and from hard sphere billiards simulation (solid) at density $\phi = 0.2$.

expect them to follow independent Poisson distributions with means $E_i$, and therefore standard deviations $\sqrt{E_i}$. Hence the standardised residuals

$$r_i = \frac{O_i - E_i}{\sqrt{E_i}}$$

should resemble independent samples from a standard normal $\mathcal{N}(0, 1)$ distribution if the fit between the hard sphere data and the Markov model is a good one. Thus we can examine the residuals and check for independence and Gaussianity as a measure of how good the Markov chain fit is.

Plots of these residuals are shown in Figures 9–11. The left figure shows $r_i$, binned in the same manner as the data in Figures 5–7, enabling the independence hypothesis to be probed. The right hand figures show a coarse histogram of the data stream $r_i$ (with 25 bins) in comparison with a unit normal, allowing the Gaussian hypothesis to be probed. These graphs are useful indicators of goodness-of-fit, although the following points should be borne in mind when intepreting them:

1. There is some slight dependence between the $r_i$ because of the constraint $\sum_i O_i = \sum_i E_i$. This dependence is negligible as each $E_i$ is a small proportion ($< 0.5\%$) of the total number of simulations.

2. The $r_i$ will be overdispersed compared to the Poisson, because of the autocorrelation. This effect should be negligible as the bins are very narrow.

3. The normality approximation is crude if $E_i$ is small, for example if $|V_k| > 4$.

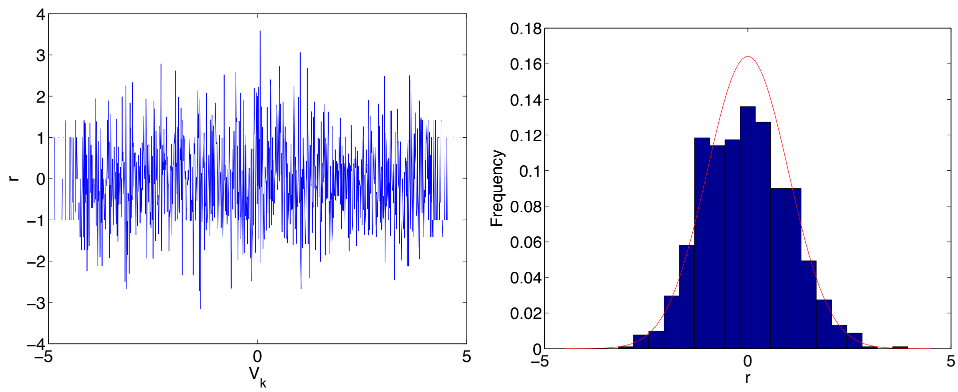


Figure 9: Comparison of the distribution of $V_k$ from the Markov chain and the hard sphere billiards simulation, at density $\phi = 0.2$.

Figure 9 shows excellent agreement between the $O_i$ and $E_i$ for $V_k$; the $r_i$ look like white noise, although the histogram shows that, because of discretisation, the distribution of $r_i$ is less peaked than $\mathcal{N}(0, 1)$.

Figure 10 shows reasonable agreement between $O_i$ and $E_i$ for $V$; the $r_i$ have a mean of roughly 0 throughout, but are underdispersed for large $|V|$ compared to $\mathcal{N}(0, 1)$, and overdispersed for $V$ around 0. Consequently the histogram of $r_i$ has slightly heavier tails than $\mathcal{N}(0, 1)$. A possible explanation for this is that it is caused by the autocorrelation in the data, but a more detailed data analysis would be required to ascertain whether this is so. Figure 11 shows some systematic bias for $T$; the $r_i$ are scattered around a mean of roughly -2 at $T = 0$, rising to 1 at $T = 1$ and then falling to a mean close to 0 for $T > 3$. This represents about a 3% discrepancy between the estimated density of $T_k$ at 0 from the Markov model and from the simulation.

The overall conclusion of these data analyses is that the fit of the hard sphere data to the Markov model is excellent at this density.

## 5.2 Density $\phi = 0.5$

The previous subsection shows that, at low densities, the Markov model is remarkably effective at capturing the effective stochastic dynamics of a single particle embedded in a gas of hard spheres. Here we extend this to higher densities, conducting experiments identical (in choice of initial data, and number of collisions) to those in the previous subsection, but with $\phi = 0.5$.

Figures 12–14 show that the velocity and collision time distributions for the hard sphere data and the Markov chain data are in close agreement.

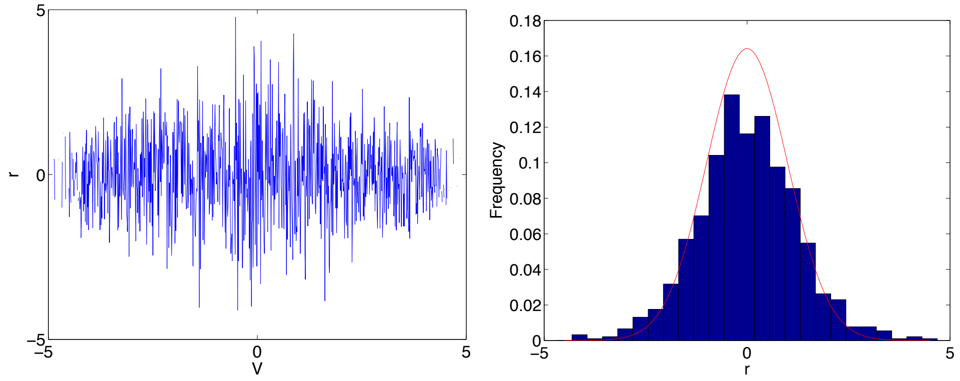


Figure 10: Comparison of the distribution of $V$ from the Markov chain and the hard spheres billiards simulation, at density $\phi = 0.2$.

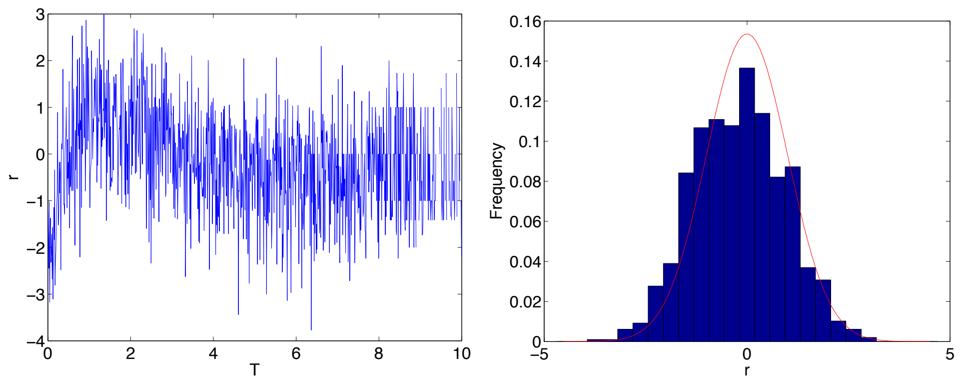


Figure 11: Comparison of the distribution of $T_k$ from the Markov chain and the hard sphere billiards simulation, at density $\phi = 0.2$.

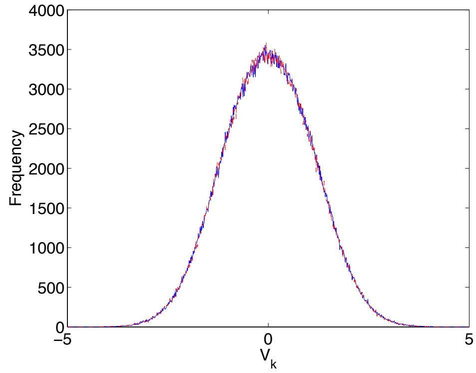


Figure 12: Distribution of $V_k$, particle velocity at collision, obtained from the Markov chain (dashed) and hard sphere billiards simulation (solid) at density $\phi = 0.5$

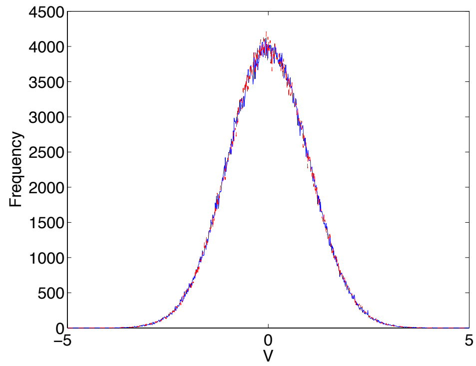


Figure 13: Distribution of $V$, particle velocity, from the Markov chain (dashed) and hard sphere billiards simulation (solid) at density $\phi = 0.5$

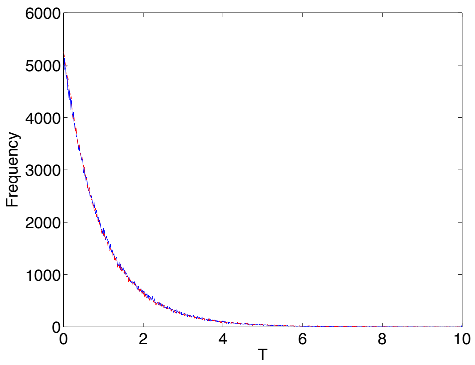


Figure 14: Distribution of $T_k$, inter-collision times from the Markov chain (dashed) and hard sphere billiards simulation (solid) at density $\phi = 0.5$.

Figures 15–17 clarify this point further: As for $\phi = 0.2$ the agreement for $V_k$ (Figure 15) is excellent apart from the effect on $r_i$ of discretisation for $|V| > 4$. The agreement for $V$ is reasonable but again shows some overdispersion for $V$ near 0, and there are small systematic differences between the two estimates for the distribution of $T$, with a very similar pattern to that for $\phi = 0.2$.

The VACF at density $\phi = 0.5$ is starting to show deviations between the hard sphere data and the Markov model; certainly the fit in Figure 18 is not as good as the fit in Figure 8. This deterioration continues as the density increases.

The overall conclusion of these data analyses is that the fit of the hard sphere data to the Markov model is very good at this density, but is notably slightly less good than at density $\phi = 0.2$.

## 5.3 Density $\phi = 0.75$

Figure 19 shows the VACF, calculated using the same number of collisions as in the previous two subsections and same initial data, for the higher density of $\phi = 0.75$. The VACF of the hard sphere model shows a negative dip, something which is impossible for a Markov model. Since our approximate model is Markovian we obtain a poor fit to the VACF of the hard sphere data.

It would be of interest to extend our model to incorporate memory effects at higher densities. We do not do this here, but we do give a survey of what has been done in this area in the next section.

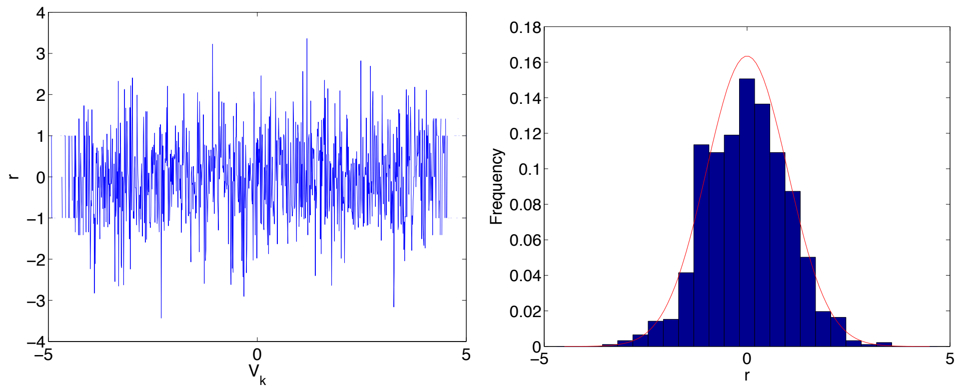


Figure 15: Comparison of the distribution of $V_k$ from the Markov chain and the hard sphere billiards simulation, at density $\phi = 0.5$.

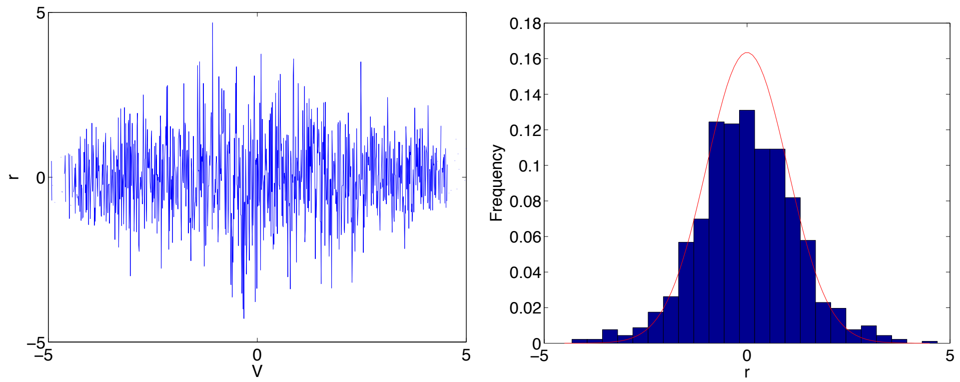


Figure 16: Comparison of the distribution of $V$ from the Markov chain and the hard spheres billiards simulation, at density $\phi = 0.5$.

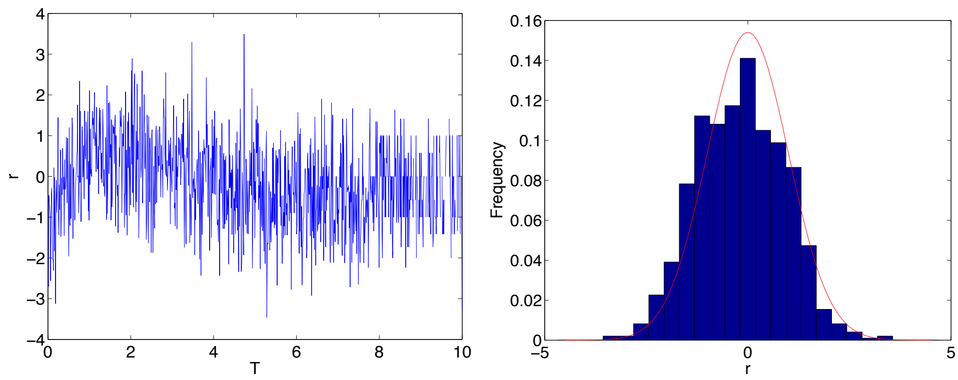


Figure 17: Comparison of the distribution of $T_k$ from the Markov chain and the hard spheres billiards simulation, at density $\phi = 0.5$.

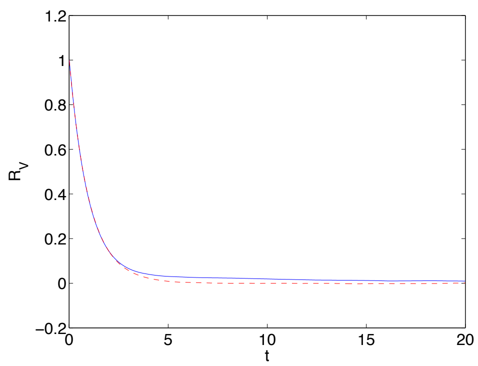


Figure 18: Velocity autocorrelation from the Markov chain (dashed) and from hard sphere billiards simulation (solid) at density $\phi = 0.5$.

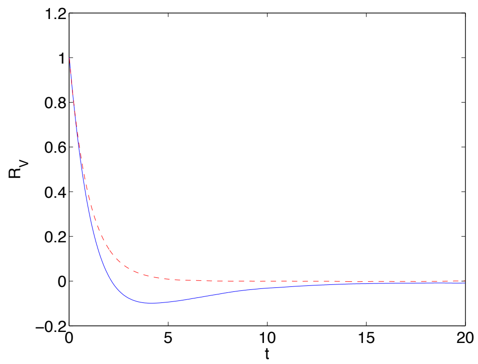


Figure 19: Velocity auto-correlation at density $\phi = 0.75$ for the Markov model (dashed) and hard spheres (solid).

# 6 Memory Effects

The previous section shows that, whilst our model is excellent at low to moderate densities, it fails to predict the hard sphere behavior well as density increase. Amongst other failures of the model, it is unable to predict the memory effect manifest in negative VACF functions at high densities. Here we briefly survey what has been done in the modelling of memory effects.

## 6.1 Markov chain models for a single particle

Burshtein, Temkin, Pasterny, and Kivelson have studied Markov chain models for the linear and angular velocity of a single particle in a rarified gas [6, 3, 4, 5, 18, 15, 2]. They are mostly concerned with reproducing the velocity autocorrelation function across a wide range of densities, in particular the negative dip observed at medium to high densities. The main difference between their approach and the approach in this paper is that the collision times are taken to be unconditionally exponential, and thus not dependent on the current particle velocity. They do not consider the ergodic properties of the chain.

They use the Keilson-Storer kernel [14], in which the probability of a post-collision velocity $v$ given that the pre-collision velocity is $v'$ is

$$\hat{f}(v, v') = f(v - \gamma v').$$

The one dimensional Maxwell distribution is conserved if

$$f(v - \gamma v') = \frac{1}{\sqrt{2\pi\sigma^2(1-\gamma^2)}} \exp\left(-\frac{(v-\gamma v')^2}{2\sigma^2(1-\gamma^2)}\right)$$

where $\sigma^2 = \langle v^2 \rangle$. This amounts to letting

$$v = \gamma v' + \sqrt{1-\gamma^2}U$$

where $U \sim \mathcal{N}(0, \sigma^2)$. As $\gamma \to 1$ collisions are weak, as $\gamma \to 0$ collisions are strong, and as $\gamma \to -1$ the velocities are anti-correlated.

Burshtein and Krongauz [3] state that the velocity autocorrelation function is known to be exponential if the distribution of the collision times is exponential and the successive values of the velocity form a Markov chain, and therefore go on to consider two different models for hard spheres fluid:

1. Non-exponential distribution of collision times.

2. Model the angle between the velocities before and after a collision, what they call the *velocity turns*, as a highly correlated Markov process.

For the first model they explore two distributions of the collision times: an interpolation of an experimentally obtained distribution of collision times, and negative $\gamma$; and using

$$\psi(t) = \frac{\exp(-t/\tau_1) - \exp(-t/\tau_2)}{\tau_1 - \tau_2} \tag{10}$$

for the collision time distribution. By using $\gamma$ close enough to $-1$ with (10) they can get a negative dip in the velocity autocorrelation function. They give some justification for using negative $\gamma$ for a heavy particle moving among a collection of light particles, but say it is not justified for particles of equal masses.

For equal masses they resort to the second model, correlated velocity turns, that is model the successive velocity turns as a Markov chain. They work in terms of the *scattering angle* $\alpha(t)$, with

$$v(t) \cdot v(0) = \|v(t)\| \|v(0)\| \cos \alpha(t).$$

A collision will result in an angle jump of $\Theta_k = \alpha(t_k+) - \alpha(t_k-)$, with probability that depends only on the last jump, $f(\Theta_k, \Theta_{k-1})$. They assume that $f(\Theta, \Theta') = f(\Theta - \Theta')$. They find that this model describes well the extent of the negative velocity correlation and location of its minimum.

## 6.2 Velocity reversing

Talbot [26] models collisions, which may or may not reverse the sign of some velocity component, and studies two simple models for fluids composed of hard particles:

1. Each particle has a constant probability $q$ of reversing direction on each collision.

2. A particle has a probability $\nu$ of reversing direction if it reversed direction on the last collision, $\mu$ otherwise.

Neither model represents the velocity autocorrelation function very accurately. The second model is able to produce negative VACF for particular values of $\mu$ and $\nu$, but the values suggested by hard sphere billiards simulation for $\mu$ and $\nu$ do not give negative VACF.

### 6.3 Enskog theory for soft potentials

Noro, Kivelson, and Tarjus [17] try to extend Enskog theory to soft potentials by a simple model for $p_r(t)$, the probability for a collision to occur at a time $t$ after the last collision. They claim it includes the "environmental crowding", softness of the potential, and correlations of successive collisions. They do not view the model above as a part of kinetic theory, and believe that correlated collision times are essential.

A collision of soft particles is defined as a velocity reversal. The time $t_r$ between collisions is the shortest time for which $v_x(0)v_x(t)$ becomes negative.

They claim their model captures much of the physics over the entire gas-liquid density range. For example, it fits $p_r(t)$ from hard sphere billiards simulations reasonably well for any temperature, density, and softness. However, their model performs poorly in describing the velocity autocorrelation function.

## 7 Conclusions

We have described a Markovian model for the motion of a single particle embedded in a hard-sphere billiard system at equilibrium. During the process of deriving and validating the model we have:

- given a rational argument for choosing inter-collision times as exponential random variables, conditional on current particle velocity;
- shown excellent agreement between the Markov model and hard sphere data, at low to moderate particle densities;
- proven that the Markov model is ergodic, with expectations converging at an exponential rate;

- surveyed existing literature on the incorporation of memory effects that arise at higher particle densities.

A natural direction in which to take this work would be to seek non-Markovian generalizations of the model used here in order to allow for memory effects at higher densities.

# A Some proofs

**Proof of Lemma 2.1** Let $F_n$ be the distribution of $Y_n$. Then

$$\begin{aligned} F_n(y) &= \Pr(Y_n \le y) = 1 - \Pr(Y_n > y) \\ &= 1 - \prod_{i=1}^{n} \Pr(nX_i > y) = 1 - (1 - F(y/n))^n. \end{aligned}$$

Since $X_i$ is a positive random variable we have $F(0) = 0$ so, by l'Hôpital,

$$\begin{aligned} \lim_{n\to\infty} \log(1 - F_n(y)) &= \lim_{\varepsilon\downarrow 0} \frac{-yF'(\varepsilon y)}{1 - F(\varepsilon y)} \\ &= -yF'(0). \end{aligned}$$

We have shown that, for fixed $y$,

$$\lim_{n\to\infty} F_n(y) = 1 - \exp(-yF'(0)) = G(y).$$

In other words that $F_n$ converges pointwise to the function $G$, which is the distribution function of an exponential distribution with parameter $F'(0)$, and hence $Y_n$ converges weakly to an exponential with parameter $\lambda = F'(0)$. □

**Proof of Theorem 2.2** From Lemma 2.1 we get that $nT$ converges weakly to an exponential random variable with parameter $\lambda = F_T'(0)$, where $F_T$ is the distribution function of $S_i$. To express $\lambda$ in terms of the velocity distribution we compute $F_T'(0)$. Denote by $F_P$ the distribution of the particle positions; by assumption it is uniform in $[-L/2, L/2]$ so $F_P' = 1/L$. Then

$$\begin{aligned} F_T(t) &= \Pr\{T < t\} = \Pr\{0 < -P/Q < t\} \\ &= \Pr\{P > 0, Q < 0, P < -tQ\} + \Pr\{P < 0, Q > 0, P > -tQ\} \\ &= \int_{q<0} f(q) \Pr\{0 < P < -tq\}\, dq + \int_{q>0} f(q) \Pr\{0 > P > -tq\}\, dq \end{aligned}$$

$$= \int\limits_{q<0} f(q)(F_P(-tq) - F_P(0))\,dq + \int\limits_{q>0} f(q)(F_P(0) - F_P(-tq))\,dq$$

so

$$\begin{aligned} F_T'(t) &= \int\limits_{q<0} f(q)(-q)F_P'(-tq)\,dq + \int\limits_{q>0} f(q)qF_P'(-tq)\,dq \\ &= \int |q|f(q)F_P'(-tq)\,dq \end{aligned}$$

and

$$F_T'(0) = \int |q|f(q)F_P'(0)\,dq = \frac{1}{L}\int |q|f(q)\,dq = \frac{1}{L}\bar{q},$$

where

$$\bar{q} := \int |q|f(q)\,dq$$

is the mean speed of the particles. Therefore

$$\lambda = nF_t'(0) = n\frac{1}{L}\bar{q} = n_0\bar{q}, \tag{11}$$

where $n_0 = n/L$ is the number density of the particles. □

# References


[1] L. Boltzmann. *Vorlesungen über Gastheorie.* Ambrosius Barth, Leipzig, 1912.

[2] A. I. Burshtein. Response to "Comment on 'Negative velocity correlation in hard sphere fluid'". In *Journal of Chemical Physics* [3], pages 9515–9516.

[3] A. I. Burshtein and M. V. Krongauz. Negative velocity correlation in hard sphere fluid. *Journal of Chemical Physics*, 102(7):2881–2887, Feb. 1995.

[4] A. I. Burshtein and A. Sivachenko. Discrimination of impact approximations for velocity and velocity sign autocorrelation functions. *Chemical Physics*, 210(3):427–433, Oct. 1996.

[5] A. I. Burshtein and A. Sivachenko. Correlation between successive velocity sign reversals within impact theory. *Chemical Physics*, 229(2–3):175–180, Apr. 1998.

[6] A. I. Burshtein and S. I. Temkin. *Spectroscopy of molecular rotation in gases and liquids*. Cambridge University Press, 1994.

[7] C. Dellago and H. Posch. Kolmogorov-Sinai entropy and Lyapunov spectra of a hard sphere gas. *Physica A*, 240(1):68–83, 1997.

[8] D. Durr, S. Goldstein, and J. Lebowitz. A mechanical model of Brownian motion. *Comm. Math. Phys.*, 78:507–530, 1981.

[9] N. Fournier and S. Méléard. Monte-Carlo approximations and fluctuations for 2D Boltzmann equations without cutoff. Preprint 601, Universités de Paris 6 & Paris 7, Laboratoire de Probabilités & Modèles Aléatoires, 4 Place Jussieu - Case 188 - 75252 Paris cedex 05, June 2000.

[10] N. Fournier and S. Méléard. A stochastic particle numerical method for 3D Boltzmann equations without cutoff. Preprint 563, Universités de Paris 6 & Paris 7, Laboratoire de Probabilités & Modèles Aléatoires, 4 Place Jussieu - Case 188 - 75252 Paris cedex 05, Feb. 2000.

[11] J. Galambos. *The asymptotic theory of extreme order statistics*. Wiley, New York, 1978.

[12] D. Givon, R. Kupferman, and A. Stuart. Extracting macroscopic dynamics: model problems and algorithms. *Nonlinearity*, 240(1):68–83, 2004.

[13] R. Holley. The motion of a heavy particle in an infinite one dimensional gas of hard spheres. *Z. Wahr. Geb.*, 17:181–219, 1971.

[14] J. Keilson and J. E. Storer. On Brownian motion, Boltzmann's equation and the Fokker-Planck equation. *Quart. Appl. Math.*, 10:243–253, 1952.

[15] D. Kivelson, J. Talbot, B. Tarjus, and J. E. Variyar. Response to "Comment on 'Negative velocity correlation in hard sphere fluid'". In *Journal of Chemical Physics* [3], page 9514.

[16] J. Mattingly, A. Stuart, and D. Higham. Ergodicity for SDEs and approximations: locally Lipschitz vector fields and degenerate noise. *Stochastic Processes and Applications*, 2001. Submitted.

[17] M. G. Noro, D. Kivelson, and G. Tarjus. A quasioscillatory collisional model for two-dimensional soft disk fluids. *Journal of Chemical Physics*, 107(18):7418–7427, Nov. 1997.

[18] K. Pasterny. Comment on "Negative velocity correlation in hard sphere fluid". In *Journal of Chemical Physics* [3], pages 9512–9513.

[19] F. Reif. *Fundamentals of Statistical and Thermal Physics*. McGraw-Hill Series in Fundamentals of Physics. McGraw-Hill, Inc., 1965.

[20] F. Rezakhanlou. Propagation of chaos for particle systems associated with discrete boltzmann equation. *Stoch. Proc. and Applics.*, 64:55–72, 1996.

[21] H. Sigurgeirsson. *Particle-field models: algorithms and applications*. PhD thesis, Stanford University, 2001.

[22] H. Sigurgeirsson, A. Stuart, and W.-L. Wan. Algorithms for particle-field simulations with collisions. *Journal of Computational Physics*, 172:766–807, 2001.

[23] D. Simanyi. The complete hyperbolicity of cylindric billiards. *Erg. Theory and Dyn. Sys.*, 22:281–302, 2002.

[24] F. Spitzer. Uniform motion with elastic collision of an infinite particle system. *Journal of Mathematics and Mechanics*, 18(10):973–989, 1969.

[25] D. Szasz, editor. *Hard ball systems and the Lorentz gas*, volume 101 of *Encyclopaedia of Mathematical Sciences*. Springer-Verlag, Berlin, 2000.

[26] J. Talbot. A statistical model for the dynamical properties of hard particle fluids. *Molecular Physics*, 75(1):43–58, 1992.

[27] H. Tanaka. Probabilistic treatment of the Boltzmann equation of Maxwellian molecules. *Z. Wahrsch. Verw. Gebiete*, 46(1):67–105, 1978.